

Long-Term Exposure to Traffic-Related Air Pollution and Noise and Dynamic Brain Connectivity across Adolescence

Mónica López-Vicente,^{1,2,3,4} Michelle Kusters,^{1,2,4} Anne-Claire Binter,^{1,2} Sami Petricola,^{1,2} Henning Tiemeier,^{4,5} Ryan Muetzel,^{4,6} and Mònica Guxens^{1,2,3,4,7}

¹ISGlobal, Barcelona, Spain

²Universitat Pompeu Fabra, Barcelona, Spain

³Spanish Consortium for Research on Epidemiology and Public Health (CIBERESP), Instituto de Salud Carlos III, Madrid, Spain

⁴Department of Child and Adolescent Psychiatry/Psychology, Erasmus University Medical Centre, Rotterdam, The Netherlands

⁵Department of Social and Behavioral Science, Harvard T.H. Chan School of Public Health, Boston, Massachusetts, USA

⁶Department of Radiology and Nuclear Medicine, Erasmus University Medical Center, Rotterdam, The Netherlands

⁷ICREA, Barcelona, Spain

BACKGROUND: Traffic-related exposures, such as air pollution and noise, show long-term associations with brain alterations in children and adolescents. The associations with functional connectivity have been studied using static approaches of resting-state functional magnetic resonance imaging (rs-fMRI) (i.e., average connectivity between regions across the scanning session).

OBJECTIVES: Our aim was to investigate the long-term association of traffic air pollution and noise during pregnancy and childhood with functional connectivity across adolescence using a dynamic approach, which captures different connectivity patterns across the scanning session.

METHODS: We used data from the Generation R population-based birth cohort. We estimated levels of 14 air pollutants and traffic noise at home addresses during pregnancy and childhood. We acquired rs-fMRI data at the age-10 y and age-14 y visits. We included participants with rs-fMRI data in at least one visit and either air pollution data ($n = 3,588$) or noise data ($n = 2,642$). We used k-means clustering to identify five connectivity patterns, called “states,” that reoccur over time and across subjects and visits. We calculated the mean time spent in each state for each participant and visit. We performed multi- and single-pollutant mixed effects models adjusted for socioeconomic and lifestyle variables, including the individual as random effect to test the associations between the exposures and the mean time spent in each state.

RESULTS: Exposure to nitrogen oxides, particulate matter (PM), and road-traffic noise was related to differences in the time spent in the connectivity states, both in the multi- and single-pollutant models. For instance, higher levels of exposure to PM with aerodynamic diameter between 2.5 μm and 10 μm ($\text{PM}_{\text{COARSE}}$) during pregnancy and higher noise exposure during childhood were associated with more time spent in a state in which the default-mode network, related to self-referential processes and mind-wandering, shows high connectivity.

DISCUSSION: Traffic-related exposures might be related to long-term alterations in brain functional network organization in adolescents. Further research should explore the potential impact of these differences on cognition and psychopathology. <https://doi.org/10.1289/EHP14525>

Introduction

Traffic-related air pollution and road traffic noise are major public health concerns in urban areas.¹ It has been shown that these environmental exposures have a negative impact on different aspects of the health of the population.^{1–3} Long-term exposure to high levels of traffic-related pollution has been associated with increased systemic inflammation that could damage the brain.^{4–6} Air pollutants might also directly affect the brain by crossing the blood–brain barrier.^{5,7} Both mechanisms activate microglia, which disrupts synapses and leads to neuronal death.^{5,8} Road traffic noise is thought to arouse the hypothalamic–pituitary–adrenal (HPA) axis

mainly through annoyance and stress.⁹ Exposures to noise and air pollution are usually correlated because they share the same source. Therefore, it is difficult to disentangle their specific effects. Nevertheless, independent associations for traffic-related air pollution and road traffic noise with cognitive outcomes have been observed.¹⁰

Long-term associations have been observed between prenatal and childhood exposures to air pollution and brain alterations in children. These brain alterations, studied using magnetic resonance imaging (MRI), include reductions of the white matter surface,¹¹ thinner cortex,^{12,13} lower restricted isotropic diffusion (a marker of white matter delayed maturation),¹⁴ and other brain structural and white matter microstructure disruptions.^{15–22} At a functional level, higher air pollution exposure has been associated with decreased brain blood flow.²² Air pollution exposure has also been related to less mature functional brain connectivity, manifested as weaker connectivity between regions belonging to the same network (within-network connectivity) and stronger connectivity between regions from different networks (between-network connectivity), indicating lower integration and lower segregation, respectively.^{23,24} In addition, changes in development of brain network connectivity, such as stronger between-network connectivity over a 2-y follow-up period at early adolescence, have recently been linked to ambient air pollution.²⁵

Research about the impact of road traffic noise exposure on the brain in humans is scarce. One study indicated that higher prenatal residential road traffic noise was associated with whole brain lower restricted isotropic diffusion at 9–12 y of age.²⁶ Another study found no associations between road traffic noise exposure at home during pregnancy and childhood periods and functional brain connectivity at 10 y of age.²⁴ A recent study, however, found that long-term exposure to road traffic noise at

Address correspondence to Mònica Guxens, Barcelona Institute for Global Health (ISGlobal) - Campus Mar, Carrer Dr. Aiguader 88, 08003 Barcelona, Spain. Email: monica.guxens@isglobal.org

Supplemental Material is available online (<https://doi.org/10.1289/EHP14525>).

The authors declare they have no conflicts of interest related to this work to disclose.

Conclusions and opinions are those of the individual authors and do not necessarily reflect the policies or views of EHP Publishing or the National Institute of Environmental Health Sciences.

EHP is a Diamond Open Access journal published with support from the NIEHS, NIH. All content is public domain unless otherwise noted. Contact the corresponding author for permission before any reuse of content. [Full licensing information](#) is available online.

Received 21 December 2023; Revised 19 February 2025; Accepted 20 March 2025; Published 5 May 2025.

Note to readers with disabilities: EHP strives to ensure that all journal content is accessible to all readers. However, some figures and Supplemental Material published in EHP articles may not conform to 508 standards due to the complexity of the information being presented. If you need assistance accessing journal content, please contact ehpsubmissions@niehs.nih.gov. Our staff will work with you to assess and meet your accessibility needs within 3 working days.

school was associated with a stronger within-network connectivity of subcortical auditory regions.²⁷

The studies that have investigated the associations of traffic-related air pollution and road traffic noise with functional brain connectivity have generally used static approaches of resting-state functional magnetic resonance imaging (rs-fMRI). This functional brain imaging modality measures the spontaneous activity of brain networks during rest. Static techniques consist of computing average correlations between the activity in different brain regions across the scanning session, assuming that the connectivity patterns are stable. However, connectivity patterns likely change within minutes, and thus applying dynamic brain connectivity techniques allows capturing different reoccurring connectivity configurations across the scanning session, usually called “states.”^{28,29} These states show different levels of organization. Older children spend more time in highly modularized connectivity patterns, which show positive within-network connectivity and negative between-network connectivity, in comparison with younger children, who spend more time in less modularized states.^{30,31} Alterations in dynamic connectivity, specifically increased time spent in disconnected or nonmodularized states, have been linked to autism spectrum disorder and schizophrenia.^{30,32}

This study aimed to explore the long-term associations of several traffic-related air pollutants and road traffic noise during pregnancy and childhood with brain dynamic functional connectivity development during adolescence. We included the following indicators of traffic-related air pollution: nitrogen dioxide (NO₂), nitrogen oxides (NO_x), particulate matter (PM) with aerodynamic diameter < 10 μm (PM₁₀) and < 2.5 μm (PM_{2.5}); PM_{COARSE} (PM_{2.5}–PM₁₀); the absorbance of PM_{2.5} fraction (PM_{2.5} absorbance) and its composition: polycyclic aromatic hydrocarbons (PAHs), organic carbon (OC), copper (Cu), iron (Fe), silicon (Si), zinc (Zn); and oxidative potential (OP) of PM_{2.5} using two acellular methods, dithiothreitol (OP^{DTT})

and electron spin resonance (OP^{ESR}). As the previous longitudinal study about air pollution and functional brain connectivity,²⁵ we focused on adolescence because it is a period of profound changes in the brain, including increases in connectivity between regions belonging to the same network and decreases in connectivity between regions from different networks.^{33,34} Long-term exposure to traffic-related air pollution and road traffic noise has been associated with systemic inflammation, which might impact the developmental rate of change (i.e., slower decrease in time spent in nonmodularized states). Deviations in typical brain developmental trajectories could represent a higher vulnerability to mental health disorders.³⁵ Based on a previous work that used data from the same cohort involved in the current study but applied a static approach of rs-fMRI,²⁴ we anticipated finding more associations with childhood exposure to air pollution than with pregnancy exposure. In the current work, we build on previous studies by adding data from a second MRI visit and using a dynamic approach of rs-fMRI. Regarding road traffic noise exposure, there is no evidence to formulate hypotheses about a differential impact of pregnancy and childhood exposure periods on brain dynamic functional connectivity development.

Methods

Participants

The current study is part of the Generation R Study, a population-based birth cohort in Rotterdam, the Netherlands.³⁶ A total of 9,901 children born between April 2002 and January 2006 were initially recruited (Figure 1). Three subjects were excluded because they requested data removal *a posteriori*. Data from twins were also excluded (*n* = 246). Air pollution data were available in 9,077 participants and noise data in 6,724 participants. We used rs-fMRI data acquired at the age-10 y visit (mean 10 y of

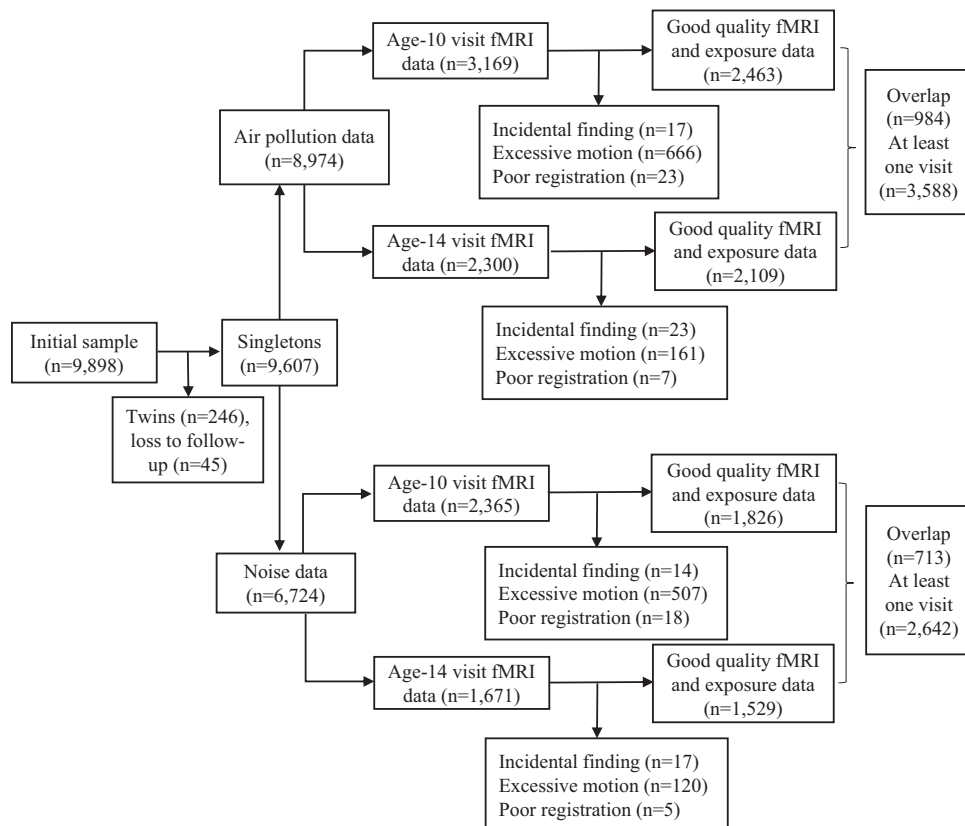


Figure 1. Flowchart of the Generation R study population.

age, range 8–12 y of age) between March 2013 and November 2015³⁷ and at the age-14 y visit (mean 14 y of age, range 13–15 y of age) between October 2016 and January 2020. A total of 8,548 participants were invited to the age-10 visit, and 7,949 were invited to the age-14 visit. From those, 3,169 participants had air pollution and rs-fMRI data at the age-10 visit; 2,365 participants had noise and rs-fMRI data at the age-10 visit; 2,300 participants had air pollution and rs-fMRI data at the age-14 visit; and 1,671 participants had noise and rs-fMRI data at the age-14 visit. The reasons for loss to follow-up included no participation in the visits, no participation in the MRI, and no acquisition of the rs-fMRI scan. We excluded participants with prominent brain imaging incidental findings or low-quality data (due to excessive motion or poor registration). In the air pollution analyses, we included 3,588 participants with good-quality rs-fMRI data in at least one visit, of which 984 had data at the two time points. In the noise analyses, we included 2,642 participants, of which 713 had data at the two time points. All parents provided written informed consent, and children provided assent (younger than 12 y of age) or consent (12 y of age or older). All study procedures were approved by the local medical ethics committee of the Erasmus University Medical Center.

Exposures

We estimated outdoor air pollution levels of 14 air pollutants using land use regression (LUR) models for each address that the participants had lived at during pregnancy (i.e., from conception to birth) and childhood (i.e., from birth to the age-10 y visit, for the participants without data at age-10 visit, the values were estimated from birth to 9 y of age) following a standardized procedure.^{38–43} In brief, in the European Study of Cohorts for Air Pollution Effects (ESCAPE) and Transport related Air Pollution and Health impacts—Integrated Methodologies for Assessing Particulate Matter (TRANSPHORM) projects, several air pollutants were monitored in various seasons between February 2009 and February 2010 in the Netherlands and Belgium. NO₂ and NO_x were measured at 80 sites. PM₁₀ and PM_{2.5} were measured at 40 sites. PM_{COARSE} was calculated by subtracting PM_{2.5} from PM₁₀. PM_{2.5} filters collected at the 40 sites were used to measure PM_{2.5} absorbance and its composition: PAHs, OC, Cu, Fe, Si, Zn. Two acellular methods were used to measure the oxidative potential of PM_{2.5}, OP^{DTT}, and OP^{ESR}. Annual mean concentrations for each pollutant were calculated and corrected for temporal variability using data from a continuous reference site. We estimated the air pollution levels at each address using LUR models. The R² cross-validation of the land use regression models is provided in Table S1. We calculated average exposure levels during pregnancy and childhood periods for each participant by weighting the exposure levels by the time spent living at each address.

The exposure to residential road traffic noise at each address was estimated using EU 2012 noise maps for five municipalities, including Rotterdam, Maassluis, Rozenburg, Schiedam, and Vlaardingen.⁴⁴ Noise maps are created every 5 y. However, we did not use the noise maps created in 2007 because of differences in the methodology. Noise was modeled using the standardized Dutch calculation methods, including polygon surfaces, buildings, barriers, slopes, crossings, and roundabouts, as well as the corresponding emission sources for each of the specific models. The maps provide a value for each polygon (corresponding to each building). The noise level at the geocoded points was determined by the noise emission of the source and other terms that denoted the attenuation from source to receiver. Noise levels were estimated at a height of 4 m at the most exposed façade of the residential addresses. We used the day–evening–night level noise indicator (L_{den}), which is the average sound level over 24 h scaled to human hearing (A-weighted). A penalty of 10 decibels (dB) for nighttime

noise (from 23:00 to 7:00) and 5 dB for evening noise (from 19:00 to 23:00) was applied to account for the greater health impacts during those hours.⁴⁵ We assumed that noise exposure levels remained relatively stable during the studied period.⁴⁶ We assigned levels of noise to each geocoded home address where the participants had lived during the study period. We calculated average noise levels for the pregnancy and the childhood periods by weighting the noise levels at each address by the time spent living at each address.

Magnetic Resonance Imaging

Magnetic resonance images were acquired on a study-dedicated 3 Tesla GE Discovery MR750w MRI System (General Electric) scanner using an 8-channel head coil. Structural T1-weighted images were obtained using a 3D coronal inversion recovery fast spoiled gradient recalled (IR-FSPGR, BRAVO) sequence using ARC acceleration. An interleaved axial echo planar imaging sequence was used to acquire 200 volumes of resting-state functional MRI data.³⁷ The resting-state scan duration was 5 min 52 s. The participants received instructions to stay awake and keep their eyes closed.

The FMRIPrep package (version 20.1.1 singularity container) was used to preprocess data.⁴⁷ For the dynamic functional connectivity analyses, we used the Group ICA Of fMRI Toolbox (GIFT) software (version 4.0b; GroupICAT) in MATLAB R2020a. In the present study, we used dynamic connectivity data computed previously using the same sample.³¹ In brief, we applied a spatially constrained group-independent component analysis, using 51 reference components grouped into 7 networks: subcortical, auditory, sensorimotor, visual, default-mode, cognitive control, and cerebellar. We computed dynamic functional network connectivity analysis between all independent components using a tapered sliding window approach. We used a window size of 25 TR (44 s) in steps of 1 TR. The alpha parameter of the Gaussian sliding window was 3 TRs. The resulting total number of windows per dataset was 171. Using data from both visits, we computed k-means clustering on the time windows from each scan to identify patterns of connectivity, called states, that reoccur over time (within the scan session) and across subjects and visits (between the scan sessions). The number of states was set to five. Three of the states were modularized, in which the components showed within- and between-network connectivity (states 1, 2, and 3), and two of the states were non- or only partially modularized states (states 4 and 5). State 1 was considered a “drowsy” state.²⁸ In this state, subcortical and sensorimotor networks showed negative connectivity. In state 2, sensorimotor and default-mode networks showed positive within-network connectivity and negative between-network connectivity. In state 3, components from the default-mode network were positively connected and they were negatively connected with components from other networks. States 2 and 3 were integrated and might indicate a higher awareness, either toward the outside stimuli (sensorimotor) or self-referential processes (default-mode). State 4 was nonmodularized, with no modular organization of functional connectivity in networks. State 5 was partially modularized, showing submodules within networks. States 4 and 5 indicated a low integration of brain networks, thus less efficiency. For each individual and visit, we obtained the mean dwell time in each dynamic state (i.e., the average time windows spent in the specific states). We transformed the mean dwell time outcomes using Box-Cox from the ‘bestNormalize’ R package because of their right-skewed distribution (Table S2 and Figure S1).

Covariates

We defined covariates *a priori* based on scientific literature and on data availability. We included participant’s age (years) at MRI assessments (continuous) and season of birth (winter, spring,

summer, and autumn). The season of birth could influence both the exposure levels and the outcomes, and participant's age is related to the outcomes. According to our theoretical framework, parental socioeconomic status would be related both to exposures and outcomes. We used multiple proxies to control as much as possible for this key confounder, including maternal education level; household income; parental national origin; maternal IQ; parental ages; marital status; parity; health-related variables, such as maternal prepregnancy body mass index (BMI), smoking, alcohol consumption, and folic acid supplement periconceptional; and neighborhood characteristics (greenness level and neighborhood socioeconomic status).

The following variables were collected by questionnaires during pregnancy (Figure S2): maternal and paternal age (continuous), education level (none or primary, secondary, and higher), national origin (Dutch, Moroccan, Surinamese, Turkish, other European, and other non-European), maternal smoking during pregnancy (never smoked during pregnancy, smoked until pregnancy was known, and continued smoking in pregnancy), maternal alcohol consumption during pregnancy [never drank during pregnancy, drank until pregnancy was known, continued drinking occasionally, and continued drinking frequently (1 glass or more per week for at least 2 trimesters)], maternal folic acid supplement (no supplement, start first 10 wk, and start periconceptional), maternal parity (no children, one child, and two or more children), marital status (married/living together, and no partner), and monthly household income (>2,200 euro; 1,600–2,200 euro; 900–1,600 euro; and <900 euro). Maternal prepregnancy BMI (continuous) was calculated based on self-reported weight and measured height. Maternal IQ (continuous) was assessed using the Raven Advanced Progressive Matrices Test at 6 y of child age.⁴⁸ Green-space exposure (continuous) was assessed using the Normalized Difference Vegetation Index (NDVI) in the surrounding area of 300 m of the home address for the pregnancy period. This index estimates the degree of land surface reflectance of light, and it was derived from the Landsat 4–5 Thematic Mapper (TM), Landsat 7 Enhanced Thematic Mapper Plus (ETM+), and Landsat 8 Operational Land Imager (OLI)/Thermal Infrared Sensor (TIRS) with 30 m × 30 m resolution.⁴⁹ The imagery had been selected according to the following criteria: cloud cover <10%, Standard Terrain Correction (Level 1T), and greenest period of the year. The socioeconomic status of the neighborhood during pregnancy (continuous), estimated using mean household income, and proportion of population with low income, low educational level, and without paid work, was provided by the National Institute of Public Health and the Environment.⁵⁰

Statistical Analyses

Missing data. The percentage of missing data in the covariates ranged between 0% (maternal age) and 36.2% (paternal education) (Excel Table S1). We imputed missing values in covariates for the sample included either in the air pollution or in the noise dataset using the EM (expectation–maximization) algorithm implemented in the R package ‘Amelia.’ We included all the exposure variables, the outcomes (mean of repeated measures or, when only one measure was available, the single available value), and all the covariates. This imputation generated one complete dataset used in all subsequent analyses.

Nonresponse analysis. We observed differences in some sociodemographic characteristics between the participants included in our study population and those excluded because of missing exposure and/or functional MRI data (Excel Table S1). For instance, the proportion of females, high parental education, high income, and Dutch origin was higher in the included sample than in the excluded sample. To correct the analyses for potential attrition

bias, we performed inverse probability weighting (IPW) for the air pollution and the noise samples independently (Table S3).

Main analyses. To assess the associations between the exposures and each dynamic connectivity outcome, we fitted linear mixed effects models using data from both MRI visits and including the child as random effect. These models account for missing data in outcomes using restricted maximum likelihood estimation. Linearity of the associations between the exposures and the outcomes was visually inspected using the R package ‘gam.’ The distributions of the model residuals were normal. We performed two sets of models for each of the exposure periods (pregnancy and childhood) and for each dynamic connectivity outcome. The first model aimed to test the overall associations between the exposures and the outcomes (MODEL_{overall}) as follows:

$$\text{Mean dwell time}_{ij} = \beta_0 + \beta_1(\text{age}) + \beta_2(\text{exposure}) + \dots + \varepsilon_{ij}, \quad (1)$$

where *Mean dwell time*_{ij} is the outcome for each dynamic connectivity state for participant *i* at visit *j*, including all covariates (indicated by “...” in the formula and described below), and residuals (ε_{ij}). The second model aimed to test associations between the exposures and changes in the developmental trajectories of the outcomes; therefore, we included the interaction between participant's age at the MRI assessment and exposure levels in each model (MODEL_{interaction}) as follows:

$$\text{Mean dwell time}_{ij} = \beta_0 + \beta_1(\text{age}) + \beta_2(\text{exposure}) + \beta_3(\text{age} \times \text{exposure}) + \dots + \varepsilon_{ij}. \quad (2)$$

All models were adjusted for the following covariates, which had <35% of missing data: participant's age at MRI assessments (centered at the average age of the first MRI assessment), season of birth, parental ages, maternal education, parental national origin, maternal smoking during pregnancy, maternal alcohol consumption during pregnancy, maternal folic acid supplement during pregnancy, maternal parity, marital status, monthly household income during pregnancy, maternal prepregnancy BMI, maternal IQ, residential surrounding greenness during pregnancy, and socioeconomic status of the neighborhood during pregnancy.

To reduce the dimension of exposures while considering correlations among them, we used the Least Absolute Shrinkage and Selection Operator (LASSO) for mixed models from the R package ‘glmLasso.’⁵¹ We chose this method because LASSO is a variable-selection model with a relatively low false discovery rate in comparison with the Bonferroni-type correction or other multipollutant models.⁵² We ran separate LASSO models for each of the two modeling strategies (MODEL_{overall} and MODEL_{interaction}). In total, we performed 20 LASSO models (2 periods × 5 outcomes × 2 modeling strategies). These models included air pollutants but not noise exposure, because the samples used were different ($n = 3,588$ for air pollution analyses and $n = 2,642$ for noise analyses). We excluded the pollutants that showed very high correlations (above 0.8) with other pollutants (i.e., NO_x, PM₁₀, PM_{2.5} absorbance, OP^{ESR}, and Fe) (Figures S3 and S4). LASSO models select the variables that best predict the outcome by penalizing certain variables of the model toward zero, based on the regularization parameters in the model (lambda parameter). We selected the lambda parameter corresponding to the lowest Bayesian Information Criterion value. Only the exposures and interaction terms between exposure and age, when applicable, were penalized in these models. The covariates were not penalized to ensure that all the models were adjusted for all the covariates. Using the R package ‘lme4,’ we then ran linear mixed effects models for each exposure selected in each LASSO model. These models

included the weights calculated using IPW. We calculated *p*-values using the function ‘Anova’ of the R package ‘car.’ The *p*-value threshold of 0.05 was corrected for the effective number of tests to correct the results for multiple testing over the five outcomes taking into account their nonindependence.⁵³ The *p*-value threshold adjusted for the effective number of tests was 0.01.

Post Hoc and Sensitivity Analyses

As a post hoc analysis, we additionally fitted single-pollutant linear mixed effects models with all the other exposures not included or selected in the LASSO models. We also performed all the analyses stratified by sex.

We included several sensitivity analyses. First, we performed all the single-pollutant models restricting the sample to participants with repeated MRI measurements ($n = 984$ for the air pollution models and $n = 713$ for the noise models). We performed different IPW for these analyses (Table S3) and included the resulting weights in the models. Second, given that the samples with repeated MRI measurements were small and they had different characteristics in comparison with the total samples (e.g., higher proportion of high maternal education level), we additionally imputed the missing outcome data using the EM algorithm and performed all the single-pollutant models including repeated measurements for all the participants. Third, we also tested the single-pollutant overall associations that were statistically significant in the main models separately per visit in linear regression models. Finally, the associations that were significant with road traffic noise in single-pollutant models were additionally adjusted for the air pollutants one by one in those participants with available air pollution and noise data ($n = 2,626$). In addition, the associations that were significant with air pollution were further adjusted for road traffic noise exposure.

All statistical analyses were performed using R statistical software (version 4.3.1; R Development Core Team).

Results

Descriptive Analyses

Half of the participants included in this study had mothers with high education levels, and the maternal national origin of 57% of the participants was the Netherlands (Table 1). During pregnancy, median NO₂ exposure levels were 34.13 μg/m³, and median PM_{2.5} levels were 16.83 μg/m³ (Table 2). During childhood, median NO₂ levels were 31.96 μg/m³ and the median PM_{2.5} levels were 16.87 μg/m³. The Spearman correlations between the pollutants in the pregnancy and childhood periods were generally moderate, ranging between 0.46 for NO₂ and 0.61 for PAH, whereas it was 0.69 for road traffic noise. Within each exposure period, the Spearman correlations among the pollutants varied, depending on the pair of pollutants. During pregnancy, NO_x, NO₂, PM₁₀, PM_{2.5}, and PM_{2.5} absorbance concentrations were highly correlated among them (ranging from 0.69 to 0.98). Other high correlations were observed among Cu, Fe, and OP^{ESR} (from 0.88 to 0.94). The correlations between road traffic noise and the air pollutants ranged between 0.14 (OC) and 0.38 (PM_{2.5} and PM_{2.5} absorbance) (Figure S3). Similar correlations were observed in the childhood period (Figure S4).

Overall Effects (MODEL_{overall})

Table 3 shows the overall associations between the average exposure levels during pregnancy and the five dynamic connectivity outcomes measured at the age-10 y and age-14 y visits. Several exposures during pregnancy were selected by the LASSO model for state 1. However, only higher exposure to NO₂ during pregnancy

was associated with more time spent in state 1 after correction for multiple testing over the outcomes [transformed mean dwell time coefficient = 0.083, 95% confidence interval (CI): 0.025, 0.141, per 10-μg/m³ increase in NO₂; $p = 0.005$]. The association is shown in the original scale of the outcome in Figure 2A. PM_{COARSE} and OP^{DTT} during pregnancy were selected by the LASSO model for time spent in state 3. After correction for multiple testing, only higher exposure to PM_{COARSE} during pregnancy was associated with more time spent in state 3 [transformed mean dwell time coefficient = 0.227 (95% CI: 0.066, 0.388) per 5-μg/m³ increase in PM_{COARSE}; $p = 0.006$; Figure 2B]. Several exposures were selected by the LASSO model for state 5; however, no significant associations were observed after correction for multiple testing. Table S4 shows the single-pollutant associations for the exposures that were not included or not selected by the LASSO.

Table 4 shows the overall associations between the average exposure levels during childhood and the five dynamic connectivity outcomes. Several exposures during childhood were selected by the LASSO models for states 1, 3, and 5. Higher exposure to NO₂ during childhood was negatively associated with time spent in state 5 after correction for multiple testing [transformed mean dwell time coefficient = -0.075 (95% CI: -0.129, -0.021) per 10-μg/m³ increase in NO₂; $p = 0.006$; Figure 2C]. Table S5 shows the single-pollutant associations for the exposures that were not included or not selected by the LASSO. Higher exposure to road traffic noise was associated with more time spent in state 3 after correction for multiple testing [transformed mean dwell time coefficient = 0.073 (95% CI: 0.022, 0.124) per 10-dB increase in road traffic noise; $p = 0.005$; Figure 2D].

Interactions with Age (MODEL_{interaction})

Interactions between age and several exposures during pregnancy and childhood were selected by the LASSO models for states 1, 4, and 5 (Tables S6 and S7). However, no significant associations remained after multiple testing corrections over the outcomes.

Analyses Stratified by Sex

The positive association between NO₂ during pregnancy and time spent in state 1 was only observed in females [transformed mean dwell time coefficient in females = 0.115 (95% CI: 0.035, 0.195) per 10-μg/m³ increase in NO₂; $p = 0.005$, and transformed mean dwell time coefficient in boys = 0.052 (95% CI: -0.034, 0.138) per 10-μg/m³ increase in NO₂; $p = 0.240$; Tables S8 and S9]. Other exposures were also selected by the LASSO for states 1 and 5, but none of them survived correction for multiple testing (Tables S10–S15).

Sensitivity Analyses

The association between exposure to PM_{COARSE} during pregnancy and time spent in state 3 remained in the models where we restricted the sample to participants with repeated MRI measurements (Table S16). The other associations did not remain significant, albeit coefficients were similar (Tables S17–S19). Results were similar when using the imputed outcome data, in comparison with the main results (Tables S20–S23). The regression models performed separately for each visit on the associations that were statistically significant in the main analyses showed no substantial differences (i.e., the coefficients were in the same direction in both visits; Table S24). The association between road traffic noise during childhood and time spent in state 3 remained after adjusting the model for the air pollutants (Table S25). Results were also comparable before and after adjusting the air pollution models for road traffic noise in the subsample with air pollution and noise data available (Table S26).

Table 1. Sociodemographic characteristics of the Generation R participants included in the air pollution and/or noise analyses of the study ($n = 3,604$).

Variables	Categories	Distribution
Participant's sex [n (%)]	Male	1,722 (47.8)
	Female	1,882 (52.2)
Maternal education level [n (%)]	High	1,816 (50.4)
	Secondary	1,508 (41.8)
Maternal national origin [n (%)]	None or primary	280 (7.8)
	the Netherlands	2,054 (57.0)
	Morocco	176 (4.9)
	Surinam	285 (7.9)
	Turkey	223 (6.2)
	Other European	281 (7.8)
	Other non-European	585 (16.2)
Paternal national origin [n (%)]	the Netherlands	2,107 (58.5)
	Morocco	200 (5.5)
	Surinam	271 (7.5)
	Turkey	230 (6.4)
	Other European	200 (5.5)
	Other non-European	596 (16.5)
	Married/living together	3,165 (87.8)
Marital status [n (%)]	No partner	439 (12.2)
	>2,200 euro	2,069 (57.4)
Monthly household income during pregnancy [n (%)]	1,600–2,200 euro	579 (16.1)
	900–1,600 euro	613 (17.0)
	<900 euro	343 (9.5)
	Never smoked during pregnancy	2,706 (75.1)
Maternal smoking during pregnancy [n (%)]	Smoked until pregnancy was known	347 (9.6)
	Continued smoking in pregnancy	551 (15.3)
	Never drank during pregnancy	1,414 (39.2)
	Drank until pregnancy was known	547 (15.2)
Maternal alcohol consumption during pregnancy [n (%)]	Continued drinking occasionally	1,306 (36.2)
	Continued drinking frequently (1 or more glass/wk for at least 2 trimesters)	337 (9.3)
	No	803 (22.3)
Folic acid supplementation during pregnancy [n (%)]	Start 1st 10 wk	1,188 (33.0)
	Start periconceptional	1,613 (44.8)
	No children	2,031 (56.4)
Parity [n (%)]	1 child	1,116 (31.0)
	2+ children	457 (12.7)
	Winter	799 (22.2)
Season of birth [n (%)]	Spring	881 (24.4)
	Summer	962 (26.7)
	Autumn	962 (26.7)
	—	10.1 ± 0.6
Participant's age at first MRI assessment [y (mean ± SD)]	—	14.0 ± 0.6
Participant's age at second MRI assessment [y (mean ± SD)]	—	3.7 ± 0.6
Years between the two MRI assessments (mean ± SD)	—	31.1 ± 4.9
Maternal age at intake [y (mean ± SD)]	—	33.7 ± 5.7
Paternal age [y (mean ± SD)]	—	23.6 ± 4.0
Maternal prepregnancy BMI [kg/m^2 (mean ± SD)]	—	97.0 ± 14.9
Maternal intelligence quotient score (mean ± SD)	—	0.4 ± 0.1
Residential surrounding greenness during pregnancy (mean ± SD)	—	-0.9 ± 1.4
Socioeconomic status neighborhood during pregnancy (mean ± SD)	—	

Note: The percentages of missing values were 8% for maternal education ($n = 288$), 2% for maternal national origin ($n = 81$), 6% for paternal national origin ($n = 215$), 8% for marital status ($n = 290$), 22% for income ($n = 801$), 12% for smoking during pregnancy ($n = 438$), 16% for alcohol consumption during pregnancy ($n = 588$), 30% for folic acid supplement ($n = 1,082$), 3% for parity ($n = 119$), 14% for paternal age ($n = 519$), 25% BMI ($n = 894$), 10% for maternal intelligence ($n = 365$), 10% for greenness ($n = 357$). —, no data; BMI, body mass index; MRI, magnetic resonance imaging; SD, standard deviation.

Discussion

Participants, mainly females, exposed to higher prenatal NO_2 levels spent more time in a drowsy state (state 1) during the scan session. Higher exposure to $\text{PM}_{\text{COARSE}}$ during pregnancy and higher exposure to road traffic noise during childhood were associated with more time spent in a default-mode network modularized state (state 3). Higher exposure to NO_2 during childhood was associated with less time spent in a partially modularized state (state 5).

Connectivity States, Traffic-Related Exposures, and Age

We found that traffic-related exposures during pregnancy and childhood were related to different patterns of functional connectivity in adolescents. Most of the findings were on the overall

associations, indicating that the exposures had a constant effect on the outcomes between the two assessments and they did not influence the rates of development. The present results indicate that higher prenatal NO_2 exposure was positively associated with spending more time in the drowsy state (state 1). In our previous study, we found that participants spent more time in the drowsy state (state 1) in the second visit (14 y of age) than in the first one (10 y of age).³¹ Another study reported that time spent in a similar state varied between healthy controls and patients with schizophrenia.³² Therefore, prenatal NO_2 exposure might interfere with the development of functional network organization. The analyses stratified by sex showed that this association was significant only in females. However, differences of effect estimates were not large, and confidence intervals overlapped, so these results should be carefully interpreted.

Table 2. Exposure levels during pregnancy and during childhood in the Generation R participants included in the air pollution ($n = 3,588$) and the noise ($n = 2,642$) analyses, and Spearman's correlations between the exposures at the two time periods.

Exposures	Pregnancy			Childhood			Spearman's correlation
	25th percentile	50th percentile	75th percentile	25th percentile	50th percentile	75th percentile	
NO ₂	31.93	34.13	36.72	28.97	31.96	35.20	0.46
NO _x	40.88	46.54	58.32	40.69	46.40	58.16	0.56
PM _{2.5}	16.58	16.83	17.23	16.58	16.87	17.44	0.57
PM _{2.5} absorbance	1.47	1.57	1.77	1.43	1.53	1.70	0.48
PM ₁₀	26.03	26.69	27.98	25.89	26.55	27.95	0.51
PM _{COARSE}	9.26	10.12	10.61	8.89	10.10	10.82	0.51
Cu	4.46	4.65	5.00	4.19	4.53	4.81	0.51
Fe	114.29	119.81	129.12	106.34	116.39	124.51	0.52
Si	87.93	88.79	90.68	87.63	88.66	90.68	0.61
Zn	17.67	18.91	21.24	17.79	19.35	22.55	0.57
OP ^{ESR}	1,001.66	1,037.16	1,103.72	971.19	1,025.39	1,091.63	0.58
OP ^{DTT}	1.26	1.35	1.40	1.15	1.22	1.28	0.56
OC	1.52	1.81	2.03	1.37	1.62	1.87	0.58
PAH	0.76	0.88	1.12	0.77	0.93	1.10	0.61
Road traffic noise	48.00	54.00	60.00	48.00	52.83	58.00	0.69

Note: Cu, elemental copper in ng/m³; Fe, elemental iron in ng/m³; NO₂, nitrogen dioxide in µg/m³; NO_x, nitrogen oxides in µg/m³; OC, organic carbon in µg/m³; OP, oxidative potential (evaluated using two acellular methods: OP^{DTT}, dithiothreitol in nmol DTT/min/m³ and OP^{ESR}, electron spin resonance in units/m³); PAHs, polycyclic aromatic hydrocarbons in ng/m³; PM, particulate matter with different aerodynamic diameters: <10 µm (PM₁₀) in µg/m³; between 10 µm and 2.5 µm (PM_{COARSE}) in µg/m³; <2.5 µm (PM_{2.5}) in µg/m³; PM_{2.5} absorbance, absorbance of PM_{2.5} filters in 10⁻⁵m⁻¹; road traffic noise, in decibels; Si, elemental silicon in ng/m³; Zn, elemental zinc in ng/m³.

Exposure to PM_{COARSE} during pregnancy and to road traffic noise during childhood were both related to spending more time in a default-mode network modularized state (state 3). This state showed positive correlations within the default-mode network components and negative correlations between this network and the others. Age was negatively associated with this state in our previous study, suggesting the associations we observed in the current study could indicate a delay in development.³¹ In line with our findings, previous research suggested that traffic-related air pollution might be related to a delay in the functional connectivity development.^{23,24} Using data from the same participants, another study found that parent-reported somatic complaints and thought problems during the 6 months before the first visit (assessed using the Child Behavior Checklist) were associated with a smaller reduction in the time spent in this state between the first and the second visits.⁵⁴ Therefore, the delay in functional connectivity development that we report in relation to PM_{COARSE} and road traffic noise might have mental health implications.

Childhood exposure to NO₂ was negatively associated with time spent in the partially modularized state (state 5). State 5 presented submodules within networks indicating low integration. Our previous publication showed negative associations between

age and this state. More time spent in state 5 in the first visit was associated with smaller decreases in parent-reported externalizing problems and attention problems between the first and the second visits.⁵⁴ Thus, the association between NO₂ and state 5 was in the opposite direction of the association we expected. Reporting observations that were similar to ours, another longitudinal study found unexpected associations between exposure to some pollutants and functional connectivity in adolescents.²⁵ Specifically, ozone was positively associated with stronger within-network connectivity, which in turn was also positively related to age. These associations could reflect compensatory mechanisms (i.e., exaggerated increase in connectivity over time because of a delay in development). These findings might indicate an alteration in the development of functional network organization with potential impact on the emergence of psychopathology, as argued by the authors.

Sensitivity analyses showed comparable results. The effect sizes observed in this study were small but similar to a 1-y change in age³¹ (i.e., around 1% decrease in time spent in state 5, both per year and per 10-µg/m³ increase in NO₂). Nitrogen oxides are more specific indicators of traffic than PM concentrations, which also originate from industry and shipping.^{38,55} However, the land use

Table 3. Associations between the exposures during pregnancy and MDT in three brain functional connectivity configurations (state 1, drowsy; state 3, default-mode network modularized; state 5, partially modularized) (MODEL_{overall}) measured at the age-10 y and/or age-14 y visit in the Generation R participants ($n = 3,588$).

Exposures	MDT (State 1)		MDT (State 3)		MDT (State 5)	
	Estimate (95% CI)	p-Value	Estimate (95% CI)	p-Value	Estimate (95% CI)	p-Value
NO ₂ (Δ 10 µg/m ³)	0.083 (0.025; 0.141)	0.005	—	—	-0.070 (-0.130; -0.010)	0.023
PM _{2.5} (Δ 5 µg/m ³)	0.117 (-0.106; 0.340)	0.305	—	—	-0.172 (-0.403; 0.059)	0.145
PM _{COARSE} (Δ 5 µg/m ³)	-0.019 (-0.167; 0.129)	0.802	0.227 (0.066; 0.388)	0.006	—	—
Cu (Δ 5 ng/m ³)	0.172 (0.013; 0.331)	0.034	—	—	—	—
Si (Δ 100 ng/m ³)	—	—	—	—	-0.152 (-0.330; 0.026)	0.094
Zn (Δ 10 ng/m ³)	0.020 (-0.046; 0.086)	0.559	—	—	-0.060 (-0.128; 0.008)	0.088
OP ^{DTT} (Δ 1 nmol DTT/min/m ³)	—	—	0.276 (0.011; 0.541)	0.041	-0.182 (-0.434; 0.070)	0.157
OC (Δ 1 µg/m ³)	0.073 (-0.000; 0.146)	0.051	—	—	—	—
PAH (Δ 1 ng/m ³)	-0.005 (-0.087; 0.077)	0.901	—	—	0.037 (-0.048; 0.122)	0.393

Note: Linear mixed effects models performed independently for each exposure/outcome, adjusted for participant's age at MRI assessments, season of birth, parental ages, maternal education, parental national origin, maternal smoking during pregnancy, maternal alcohol consumption during pregnancy, maternal folic acid supplement during pregnancy, maternal parity, marital status, monthly household income during pregnancy, maternal prepregnancy body mass index, maternal IQ, green space during pregnancy and socioeconomic status of the neighborhood during pregnancy. All shown associations were selected by the LASSO. In bold, associations that survived multiple testing correction over the outcomes ($p < 0.01$). The associations are shown in Figure 2. —, no data; CI, confidence interval; Cu, elemental copper; MDT, mean dwell time; MRI, magnetic resonance imaging; NO₂, nitrogen dioxide; OC, organic carbon; OP^{DTT}, oxidative potential (evaluated using dithiothreitol); PAHs, polycyclic aromatic hydrocarbons; PM, particulate matter with different aerodynamic diameters: between 10 µm and 2.5 µm (PM_{COARSE}); <2.5 µm (PM_{2.5}); Si, elemental silicon; Zn, elemental zinc.

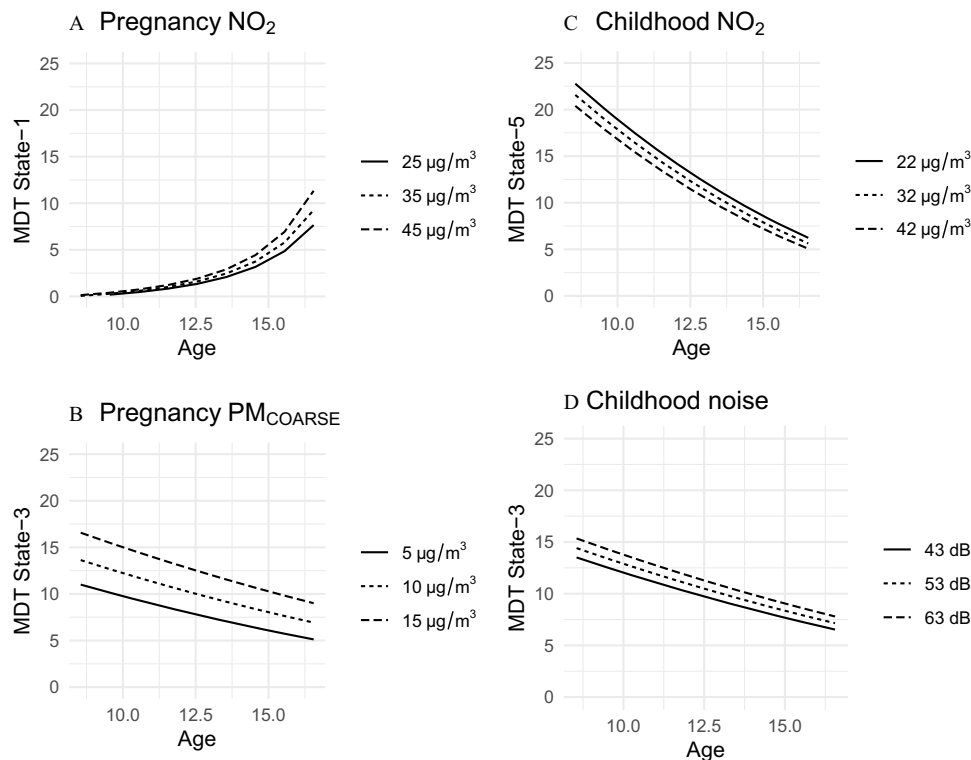


Figure 2. Associations between traffic-related exposures (air pollution and noise) and mean dwell time (MDT, number of time windows) in three brain functional connectivity configurations (state 1, drowsy; state 3, default-mode network modularized; state 5, partially modularized) in the Generation R participants ($n = 3,588$ for air pollutants and $n = 2,642$ for noise). Note: Linear mixed effects models performed independently for each exposure/outcome, adjusted for participant's age at MRI assessments, season of birth, parental ages, maternal education, parental national origin, maternal smoking during pregnancy, maternal alcohol consumption during pregnancy, maternal folic acid supplement during pregnancy, maternal parity, marital status, monthly household income during pregnancy, maternal prepregnancy BMI, maternal IQ, green space during pregnancy and socioeconomic status of the neighborhood during pregnancy. The OP^{ESR} model additionally included age interaction. This figure only represents the associations that were selected by the LASSO (road traffic noise was not included) and that survived multiple testing correction over the outcomes ($p < 0.01$). The exposure levels represent the mean, one unit (Δ) decrease and increase. This categorization was performed for depiction purposes only. Associations are reported in Tables 3 and 4 and Table S5. BMI, body mass index; NO_2 , nitrogen dioxide; PM, particulate matter; PM_{COARSE} , PM with aerodynamic diameter between 10 μm and 2.5 μm .

regression models used in this study were developed to estimate traffic-related air pollution only. Therefore, our findings provide new evidence about the influence of traffic-related air pollution and road traffic noise exposures on the functional brain connectivity of adolescents. The fact that we generally observed differences in the functional connectivity organization that are constant over time ($MODEL_{overall}$), rather than differences in the

developmental rates ($MODEL_{interaction}$), suggests that the brains of highly exposed individuals are differently wired in comparison with less-exposed individuals. However, it is also possible that we were not able to capture differences in rates of development due to the period of outcome measurement, and this might be different for other periods (i.e., highly exposed individuals might show a catch-up). Therefore, the long-term effects of traffic exposures on

Table 4. Associations between the exposures during childhood and MDT in three brain functional connectivity configurations (state 1, drowsy; state 3, default-mode network modularized; state 5, partially modularized) ($MODEL_{overall}$) measured at the age-10 y and/or age-14 y visit in the Generation R participants ($n = 3,588$).

Exposures	MDT (State 1)		MDT (State 3)		MDT (State 5)	
	Estimate (95% CI)	<i>p</i> -Value	Estimate (95% CI)	<i>p</i> -Value	Estimate (95% CI)	<i>p</i> -Value
NO_2 ($\Delta 10 \mu g/m^3$)	-0.002 (-0.054; 0.050)	0.936	—	—	-0.075 (-0.129; -0.021)	0.006
$PM_{2.5}$ ($\Delta 5 \mu g/m^3$)	-0.073 (-0.291; 0.145)	0.509	—	—	—	—
PM_{COARSE} ($\Delta 5 \mu g/m^3$)	-0.007 (-0.131; 0.117)	0.918	0.131 (-0.004; 0.266)	0.056	-0.128 (-0.256; 0.000)	0.051
Cu ($\Delta 5 ng/m^3$)	—	—	—	—	-0.116 (-0.306; 0.074)	0.233
Si ($\Delta 100 ng/m^3$)	—	—	—	—	-0.196 (-0.435; 0.043)	0.107
Zn ($\Delta 10 ng/m^3$)	—	—	—	—	-0.026 (-0.081; 0.029)	0.360
OP^{DTT} ($\Delta 1 nmol DTT/min/m^3$)	—	—	—	—	-0.012 (-0.287; 0.263)	0.934
OC ($\Delta 1 \mu g/m^3$)	0.083 (0.009; 0.157)	0.029	—	—	-0.071 (-0.148; 0.006)	0.070
PAH ($\Delta 1 ng/m^3$)	-0.128 (-0.245; -0.011)	0.032	0.160 (0.033; 0.287)	0.014	0.130 (0.009; 0.251)	0.035

Note: Linear mixed effects models performed independently for each exposure/outcome, adjusted for participant's age at MRI assessments, season of birth, parental ages, maternal education, parental national origin, maternal smoking during pregnancy, maternal alcohol consumption during pregnancy, maternal folic acid supplement during pregnancy, maternal parity, marital status, monthly household income during pregnancy, maternal prepregnancy body mass index, maternal IQ, green space during pregnancy and socioeconomic status of the neighborhood during pregnancy. All shown associations were selected by the LASSO. In bold, associations that survived multiple testing correction over the outcomes ($p < 0.01$). The associations are shown in Figure 2. —, no data; CI, confidence interval; Cu, elemental copper; MDT, mean dwell time; MRI, magnetic resonance imaging; NO_2 , nitrogen dioxide; OC, organic carbon; OP^{DTT} , oxidative potential (evaluated using dithiothreitol); PAHs, polycyclic aromatic hydrocarbons; PM, particulate matter with different aerodynamic diameters: between 10 μm and 2.5 μm (PM_{COARSE}); <2.5 μm ($PM_{2.5}$); Si, elemental silicon; Zn, elemental zinc.

brain dynamic connectivity during childhood and late adolescence remain to be explored.

Biological Mechanisms

Resting-state networks are generally established during the third trimester of gestation at different rates.⁵⁶ During childhood, networks supporting motor and sensory processes show a robust functional organization, whereas default-mode network and other networks involved in higher-order cognitive functions are less mature.⁵⁷ Exposure to traffic-related pollutants and noise could disrupt the development of functional connectivity both during pregnancy and childhood periods; however, the networks affected would likely differ depending on the exposure period. Biological mechanisms by which the traffic-related exposures may affect the brain involve dysfunction of the HPA axis, inflammation, and oxidative stress processes.^{4,9} Researchers have hypothesized that air pollutants may interact with the blood–brain barrier cells, causing alterations in their function and producing pro-inflammatory signals.^{5,7} Microglia respond to these signals, promoting neuronal death and synaptic toxicity.^{5,8} Air pollutants have also been shown to modulate the expression of genes related to vasoregulatory pathways in the brain in animal studies.⁵⁸

Limitations

Several limitations related to this study should be considered. We were not able to extrapolate the levels of pollutants to the periods of interest because historical data from monitoring stations were not available for all pollutants. Therefore, we assumed that the pollutant concentrations remained spatially stable over time.⁵⁹ Regarding the noise exposure, we used 2012 noise maps, assuming that noise exposure levels remained relatively stable during the studied periods.⁴⁶ In addition, we used only average noise over 24 h, whereas other noise indicators, such as those related to fluctuations, have been demonstrated to be related to cognitive performance.⁶⁰ In this study, we considered only the exposure levels at home addresses, although exposure during commuting and at school represent the highest percentage of the total daily pollutant dose received,⁶¹ and traffic-related exposure at school has previously been linked to brain function.^{23,27} Regarding the rs-fMRI data acquisition, a longer scan duration would have resulted in a more accurate characterization of the dynamic states. However, a scan duration of 5–6 min is commonly used, has previously been shown to yield replicable outcomes, and ensures high quality data and minimized burden on our young participants.^{30,62–64} Another limitation of our study is the loss of participants. The differences in the sociodemographic characteristics of the participants included in our analyses and those excluded due to a missing exposure and/or functional MRI data could have caused selection bias. This factor was particularly important for the noise analyses, in which we did not have data for those participants who moved out of the municipalities with available noise data. Yet, we implemented inverse probability weighting in an attempt to reduce the risk of attrition bias. Finally, the number of participants with repeated measures of the outcome was relatively low. Nevertheless, the mixed effects models partially addressed this limitation by handling the missing outcome data, and the models performed using imputed outcome data indicated consistent findings.

Strengths

This study has several strengths, such as the large sample based on the general population. Regarding the exposures, we used standardized and validated models to estimate the exposure levels individually for each participant during the prenatal and

childhood periods, accounting for changes of residence. Moreover, our study was comprehensive in terms of the large number of air pollutants included, while accounting for the interdependence among them by using multipollutant models. The longitudinal design of the study including two repeated MRI measures, which increased the power of the analyses, is unique in this field. In addition, we used a novel approach to explore brain functional connectivity. Functional MRI analyses, and resting-state in particular, are considerably sensitive to motion. In addition to excluding data with excessive motion applying a strict threshold, the dynamic connectivity approach that we took also contributed to reducing the impact of motion in our analyses. This method allowed us to split the MRI assessment in very short windows of time and cluster the data in different connectivity configurations. Therefore, the brain activity could be better disentangled from the noise signal and other types of signals.

Conclusion

To conclude, our findings suggest that traffic-related exposures might be related to long-term alterations in brain functional network organization in adolescents. The differences were generally stable in time, suggesting that the exposures did not influence developmental rates of brain dynamic connectivity over the studied period. Further research should explore different developmental periods, such as childhood and late adolescence, as well as the potential impact of these differences on cognition and psychopathology.

Acknowledgments

The authors gratefully acknowledge the contribution of children and parents, general practitioners, hospitals, midwives, and pharmacies in Rotterdam.

This study was supported by the Project IJC2020-045355-I, funded by MCIN/AEI/10.13039/501100011033 and by the European Union NextGenerationEU/PRTR (M.L.-V.). This study was co-financed by the Agencia Estatal de Investigación (AEI) and the European Social Fund (FSE) “EL FSE invierte en tu futuro” with reference number PRE2020-092005, according to the Resolution of the Presidency of the AEI, by which grants are awarded for predoctoral contracts for the training of doctors, call 2020 (M.K.). This study received funding from the European Union’s Horizon 2020 research and innovation program under grant agreement No. 874583 (ATHLETE project, A.B.).

This publication reflects only the authors’ view, and the European Commission is not responsible for any use that may be made of the information it contains. Generation R Neuroimaging was supported by the Sophia Foundation project S18–20 (R.L.M.), the Erasmus MC Fellowship (R.L.M.), The Netherlands Organization for Scientific Research (2021.042, Snellius, R.L.M.), and the Netherlands Organization for Health Research and Development (ZonMw) Vici project 016.VICI.170.200 (H.T.). M.G. was funded by a Miguel Servet II fellowship (CPII18/00018) from the Spanish Institute of Health Carlos III. The Generation R Study is conducted by the Erasmus MC in close collaboration with Faculty of Social Sciences of the Erasmus University Rotterdam; the Municipal Health Service Rotterdam area, Rotterdam; and the Stichting Trombosedienst & Artsenlaboratorium Rijnmond (STAR-MDC), Rotterdam. The geocodification of the addresses of the study participants and the air pollution estimations were done within the framework of a project funded by the Health Effects Institute (HEI) (Assistance Award No. R-82811201) and by the Spanish Institute of Health Carlos III (PI20/01695 including FEDER funds). The authors acknowledge the E-OBS dataset from the EU-FP6 project UERRA (<https://www.uerra.eu>) and the

Copernicus Climate Change Service, and the data providers in the ECA&D project (<https://www.ecad.eu>). The authors acknowledge support from the grant CEX2023-0001290-S funded by MCIN/AEI/10.13039/501100011033, the Generalitat de Catalunya through the CERCA Program, and the Ministry of Research and Universities of the Government of Catalonia (2021 SGR 01564).

References

- Hänninen O, Knol AB, Jantunen M, Lim T-A, Conrad A, Rappolder M, et al. 2014. Environmental burden of disease in Europe: assessing nine risk factors in six countries. *Environ Health Perspect* 122(5):439–446, PMID: 24584099, <https://doi.org/10.1289/ehp.1206154>.
- Rojas-Rueda D, Morales-Zamora E, Alsufyani WA, Herbst CH, AlBalawi SM, Alsukait R, et al. 2021. Environmental risk factors and health: an umbrella review of meta-analyses. *Int J Environ Res Public Health* 18(2):704, PMID: 33467516, <https://doi.org/10.3390/ijerph18020704>.
- Stansfeld SA. 2015. Noise effects on health in the context of air pollution exposure. *Int J Environ Res Public Health* 12(10):12735–12760, PMID: 26473905, <https://doi.org/10.3390/ijerph121012735>.
- Thomson EM. 2019. Air pollution, stress, and allostatic load: linking systemic and Central nervous system impacts. *J Alzheimers Dis* 69(3):597–614, PMID: 31127781, <https://doi.org/10.3233/JAD-190015>.
- Block ML, Calderón-Garcidueñas L. 2009. Air pollution: mechanisms of neuroinflammation and CNS disease. *Trends Neurosci* 32(9):506–516, PMID: 19716187, <https://doi.org/10.1016/j.tins.2009.05.009>.
- Costa LG, Cole TB, Coburn J, Chang YC, Dao K, Roqué PJ. 2017. Neurotoxicity of traffic-related air pollution. *Neurotoxicology* 59:133–139, PMID: 26610921, <https://doi.org/10.1016/j.neuro.2015.11.008>.
- Calderón-Garcidueñas L, Solt AC, Henríquez-Roldán C, Torres-Jardón R, Nuse B, Herritt L, et al. 2008. Long-term air pollution exposure is associated with neuroinflammation, an altered innate immune response, disruption of the blood–brain barrier, ultrafine particulate deposition, and accumulation of amyloid beta-42 and alpha-synuclein in children and young adults. *Toxicol Pathol* 36(2):289–310, PMID: 18349428, <https://doi.org/10.1177/0192623307313011>.
- Davis DA, Akopian G, Walsh JP, Sioutas C, Morgan TE, Finch CE. 2013. Urban air pollutants reduce synaptic function of CA1 neurons via an NMDA/N_D pathway in vitro. *J Neurochem* 127(4):509–519, PMID: 23927064, <https://doi.org/10.1111/jnc.12395>.
- Münzel T, Kröller-Schön S, Oelze M, Gori T, Schmidt FP, Steven S, et al. 2020. Adverse cardiovascular effects of traffic noise with a focus on nighttime noise and the new WHO noise guidelines. *Annu Rev Public Health* 41:309–328, PMID: 31922930, <https://doi.org/10.1146/annurev-publhealth-081519-062400>.
- van Kempen E, Fischer P, Janssen N, Houthuijs D, van Kamp I, Stansfeld S, et al. 2012. Neurobehavioral effects of exposure to traffic-related air pollution and transportation noise in primary schoolchildren. *Environ Res* 115:18–25, PMID: 22483436, <https://doi.org/10.1016/j.envres.2012.03.002>.
- Peterson BS, Rauh VA, Bansal R, Hao X, Toth Z, Nati G, et al. 2015. Effects of prenatal exposure to air pollutants (polycyclic aromatic hydrocarbons) on the development of brain white matter, cognition, and behavior in later childhood. *JAMA Psychiatry* 72(6):531–540, PMID: 25807066, <https://doi.org/10.1001/jamapsychiatry.2015.57>.
- Guxens M, Lubczyńska MJ, Muetzel RL, Dalmau-Bueno A, Jaddoe VVV, Hoek G, et al. 2018. Air pollution exposure during fetal life, brain morphology, and cognitive function in school-age children. *Biol Psychiatry* 84(4):295–303, PMID: 29530279, <https://doi.org/10.1016/j.biopsych.2018.01.016>.
- Lubczyńska MJ, Muetzel RL, El Marroun H, Hoek G, Kooter IM, Thomson EM, et al. 2021. Air pollution exposure during pregnancy and childhood and brain morphology in preadolescents. *Environ Res* 198:110446, PMID: 33221303, <https://doi.org/10.1016/j.envres.2020.110446>.
- Lubczyńska MJ, Muetzel RL, El Marroun H, Basagaña X, Strak M, Denault W, et al. 2020. Exposure to air pollution during pregnancy and childhood, and white matter microstructure in preadolescents. *Environ Health Perspect* 128(2):027005, PMID: 32074458, <https://doi.org/10.1289/EHP4709>.
- Calderón-Garcidueñas L, Engle R, Mora-Tiscareño A, Styner M, Gómez-Garza G, Zhu H, et al. 2011. Exposure to severe urban air pollution influences cognitive outcomes, brain volume and systemic inflammation in clinically healthy children. *Brain Cogn* 77(3):345–355, PMID: 22032805, <https://doi.org/10.1016/j.bandc.2011.09.006>.
- Calderón-Garcidueñas L, Mora-Tiscareño A, Ontiveros E, Gómez-Garza G, Barragán-Mejía G, Broadway J, et al. 2008. Air pollution, cognitive deficits and brain abnormalities: a pilot study with children and dogs. *Brain Cogn* 68(2):117–127, PMID: 18550243, <https://doi.org/10.1016/j.bandc.2008.04.008>.
- Pujol J, Fenoll R, Macià D, Martínez-Vilavella G, Alvarez-Pedrerol M, Rivas I, et al. 2016. Airborne copper exposure in school environments associated with poorer motor performance and altered basal ganglia. *Brain Behav* 6(6):e00467, PMID: 27134768, <https://doi.org/10.1002/brb3.467>.
- Beckwith T, Cecil K, Altaye M, Severs R, Wolfe C, Percy Z, et al. 2020. Reduced gray matter volume and cortical thickness associated with traffic-related air pollution in a longitudinally studied pediatric cohort. *PLoS One* 15(1):e0228092, PMID: 31978108, <https://doi.org/10.1371/journal.pone.0228092>.
- Cserbik D, Chen J-C, McConnell R, Berhane K, Sowell ER, Schwartz J, et al. 2020. Fine particulate matter exposure during childhood relates to hemispheric-specific differences in brain structure. *Environ Int* 143:105933, PMID: 32659528, <https://doi.org/10.1016/j.envint.2020.105933>.
- Mortamais M, Pujol J, Martínez-Vilavella G, Fenoll R, Reynes C, Sabatier R, et al. 2019. Effects of prenatal exposure to particulate matter air pollution on corpus callosum and behavioral problems in children. *Environ Res* 178:108734, PMID: 31539824, <https://doi.org/10.1016/j.envres.2019.108734>.
- Burnor E, Cserbik D, Cotter DL, Palmer CE, Ahmadi H, Eckel SP, et al. 2021. Association of outdoor ambient fine particulate matter with intracellular white matter microstructural properties among children. *JAMA Netw Open* 4(12):e2138300, PMID: 34882178, <https://doi.org/10.1001/jamanetworkopen.2021.38300>.
- Peterson BS, Bansal R, Sawardekar S, Nati C, Elgalalawy ER, Hoepner LA, et al. 2022. Prenatal exposure to air pollution is associated with altered brain structure, function, and metabolism in childhood. *J Child Psychol Psychiatry* 63(11):1316–1331, PMID: 35165899, <https://doi.org/10.1111/jcpp.13578>.
- Pujol J, Martínez-Vilavella G, Macià D, Fenoll R, Alvarez-Pedrerol M, Rivas I, et al. 2016. Traffic pollution exposure is associated with altered brain connectivity in school children. *Neuroimage* 129:175–184, PMID: 26825441, <https://doi.org/10.1016/j.neuroimage.2016.01.036>.
- Pérez-Crespo L, Kusters MSW, López-Vicente M, Lubczyńska MJ, Foraster M, White T, et al. 2022. Exposure to traffic-related air pollution and noise during pregnancy and childhood, and functional brain connectivity in preadolescents. *Environ Int* 164:107275, PMID: 35580436, <https://doi.org/10.1016/j.envint.2022.107275>.
- Cotter DL, Campbell CE, Sukumaran K, McConnell R, Berhane K, Schwartz J, et al. 2023. Effects of ambient fine particulates, nitrogen dioxide, and ozone on maturation of functional brain networks across early adolescence. *Environ Int* 177:108001, PMID: 37307604, <https://doi.org/10.1016/j.envint.2023.108001>.
- Binter A, Granés L, Bannier E, Castro Md, Petricola S, Fossati S, et al. 2024. Urban environment during pregnancy and childhood and white matter microstructure in preadolescence in two European birth cohorts. *Environ Pollut* 346:123612, PMID: 38387546, <https://doi.org/10.1016/j.envpol.2024.123612>.
- Martínez-Vilavella G, Pujol J, Blanco-Hinojo L, Deus J, Rivas I, Persavento C, et al. 2023. The effects of exposure to road traffic noise at school on central auditory pathway functional connectivity. *Environ Res* 226:115574, PMID: 36841520, <https://doi.org/10.1016/j.envres.2023.115574>.
- Allen EA, Damaraju E, Plis SM, Erhardt EB, Eichele T, Calhoun VD. 2014. Tracking whole-brain connectivity dynamics in the resting state. *Cereb Cortex* 24(3):663–676, PMID: 23146964, <https://doi.org/10.1093/cercor/bhs352>.
- Calhoun VD, Miller R, Pearlson G, Adali T. 2014. The chronnectome: time-varying connectivity networks as the next frontier in fMRI data discovery. *Neuron* 84(2):262–274, PMID: 25374354, <https://doi.org/10.1016/j.neuron.2014.10.015>.
- Rashid B, Blanken LME, Muetzel RL, Miller R, Damaraju E, Arbabshirani MR, et al. 2018. Connectivity dynamics in typical development and its relationship to autistic traits and autism spectrum disorder. *Hum Brain Mapp* 39(8):3127–3142, PMID: 29602272, <https://doi.org/10.1002/hbm.24064>.
- López-Vicente M, Agcaoglu O, Pérez-Crespo L, Estévez-López F, Heredia-Genestar JM, Mulder RH, et al. 2021. Developmental changes in dynamic functional connectivity from childhood into adolescence. *Front Syst Neurosci* 15:724805, PMID: 34880732, <https://doi.org/10.3389/fnsys.2021.724805>.
- Damaraju E, Allen EA, Belger A, Ford JM, McEwen S, Mathalon DH, et al. 2014. Dynamic functional connectivity analysis reveals transient states of dysconnectivity in schizophrenia. *Neuroimage Clin* 5:298–308, PMID: 25161896, <https://doi.org/10.1016/j.nicl.2014.07.003>.
- Luciana M. 2013. Adolescent brain development in normality and psychopathology. *Dev Psychopathol* 25(4 pt 2):1325–1345, PMID: 24342843, <https://doi.org/10.1017/S0954579413000643>.
- Vása F, Romero-García R, Kitzbichler MG, Seidlitz J, Whitaker KJ, Vaghi MM, et al. 2020. Conservative and disruptive modes of adolescent change in human brain functional connectivity. *Proc Natl Acad Sci USA* 117(6):3248–3253, PMID: 31992644, <https://doi.org/10.1073/pnas.1906144117>.
- Crone EA, Elzinga BM. 2015. Changing brains: how longitudinal functional magnetic resonance imaging studies can inform us about cognitive and social-affective growth trajectories. *Wiley Interdiscip Rev Cogn Sci* 6(1):53–63, PMID: 26262928, <https://doi.org/10.1002/wics.1327>.
- Kooijman MN, Kruitthof CJ, van Duijn CM, Duijts L, Franco OH, van IJendoorn MH, et al. 2016. The Generation R study: design and cohort update 2017. *Eur J Epidemiol* 31(12):1243–1264, PMID: 28070760, <https://doi.org/10.1007/s10654-016-0224-9>.
- White T, Muetzel RL, El Marroun H, Blanken LME, Jansen P, Bolhuis K, et al. 2018. Paediatric population neuroimaging and the Generation R Study: the

- second wave. *Eur J Epidemiol* 33(1):99–125, PMID: 29064008, <https://doi.org/10.1007/s10654-017-0319-y>.
38. Beelen R, Hoek G, Vienneau D, Eeftens M, Dimakopoulou K, Pedeli X, et al. 2013. Development of NO₂ and NO_x land use regression models for estimating air pollution exposure in 36 study areas in Europe – the ESCAPE project. *Atmos Environ* 72:10–23, <https://doi.org/10.1016/j.atmosenv.2013.02.037>.
 39. Eeftens M, Beelen R, de Hoogh K, Bellander T, Cesaroni G, Cirach M, et al. 2012. Development of land use regression models for PM(2.5), PM(2.5) absorbance, PM(10) and PM(coarse) in 20 European study areas; results of the ESCAPE project. *Environ Sci Technol* 46(20):11195–11205, PMID: 22963366, <https://doi.org/10.1021/es301948k>.
 40. de Hoogh K, Wang M, Adam M, Badaloni C, Beelen R, Birk M, et al. 2013. Development of land use regression models for particle composition in twenty study areas in Europe. *Environ Sci Technol* 47(11):5778–5786, PMID: 23651082, <https://doi.org/10.1021/es400156t>.
 41. Jedynska A, Hoek G, Wang M, Eeftens M, Cyrus J, Keuken M, et al. 2014. Development of land use regression models for elemental, organic carbon, PAH, and hopanes/steranes in 10 ESCAPE/TRANSPHORM European study areas. *Environ Sci Technol* 48(24):14435–14444, PMID: 25317817, <https://doi.org/10.1021/es502568z>.
 42. Yang A, Wang M, Eeftens M, Beelen R, Dons E, Leseman DLAC, et al. 2015. Spatial variation and land use regression modeling of the oxidative potential of fine particles. *Environ Health Perspect* 123(11):1187–1192, PMID: 25840153, <https://doi.org/10.1289/ehp.1408916>.
 43. Guxens M, Lubczynska MJ, Perez-Crespo L, Muetzel RL, El Marroun H, Basagaña X, et al. 2022. Associations of air pollution on the brain in children: a brain imaging study. *Res Rep Health Eff Inst* 2022(209):1–61, PMID: 36106707.
 44. European Commission. 2002. European Environmental Noise Directive. Directive 2002/49/EC of the European Parliament and of the Council of 25 June 2002. <https://eur-lex.europa.eu/legal-content/EN/TXT/PDF/?uri=CELEX:32002L0049> [accessed 29 April 2025].
 45. World Health Organization. 2018. *Environmental Noise Guidelines for the European Region*. <https://iris.who.int/bitstream/handle/10665/279952/9789289053563-eng.pdf?sequence=1> [accessed 29 April 2025].
 46. European Environment Agency. 2020. Environmental Noise in Europe – 2020. <https://www.eea.europa.eu/en/analysis/publications/environmental-noise-in-europe> [accessed 29 April 2025].
 47. Esteban O, Markiewicz CJ, Blair RW, Moodie CA, Isik AI, Erramuzpe A, et al. 2019. fMRIprep: a robust preprocessing pipeline for functional MRI. *Nat Methods* 16(1):111–116, PMID: 30532080, <https://doi.org/10.1038/s41592-018-0235-4>.
 48. Raven JC. 1962. *Advanced Progressive Matrices*. London, UK: H. K. Lewis & Co. Ltd.
 49. Rhew IC, Vander Stoep A, Kearney A, Smith NL, Dunbar MD. 2011. Validation of the normalized difference vegetation index as a measure of neighborhood greenness. *Ann Epidemiol* 21(12):946–952, PMID: 21982129, <https://doi.org/10.1016/j.annepidem.2011.09.001>.
 50. NIPHE (National Institute for Public Health and the Environment). 2017. Sociaaleconomische Status 2017. <https://www.volksgezondheidenzorg.info/onderwerp/sociaaleconomische-status/regionaal-internationaal/node-sociaaleconomische-status> [accessed 19 May 2021].
 51. Tibshirani R. 1996. Regression shrinkage and selection via the lasso. *Journal of the Royal Statistical Society Series B (Methodological)* 58(1):267–288, <https://doi.org/10.1111/j.2517-6161.1996.tb02080.x>.
 52. Agier L, Portengen L, Chadeau-Hyam M, Basagaña X, Giorgis-Allemand L, Siroux V, et al. 2016. A systematic comparison of linear regression-based statistical methods to assess exposome–health associations. *Environ Health Perspect* 124(12):1848–1856, PMID: 27219331, <https://doi.org/10.1289/EHP172>.
 53. Galwey NW. 2009. A new measure of the effective number of tests, a practical tool for comparing families of non-independent significance tests. *Genet Epidemiol* 33(7):559–568, PMID: 19217024, <https://doi.org/10.1002/gepi.20408>.
 54. Dall’Aglio L, Estévez-López F, López-Vicente M, Xu B, Agcaoglu O, Boroda E, et al. 2023. Exploring the longitudinal associations of functional network connectivity and psychiatric symptom changes in youth. *Neuroimage Clin* 38:103382, PMID: 36965455, <https://doi.org/10.1016/j.nicl.2023.103382>.
 55. Thunis P, Pisoni E, Zauli Sajani S, Monforti F, Bessagnet B, Vignati E, et al. 2023. *Urban PM2.5 Atlas. Air Quality in European Cities–2023 Report*. Luxembourg: Publications Office of the European Union. <https://doi.org/10.2760/63641>.
 56. Doria V, Beckmann CF, Arichi T, Merchant N, Groppo M, Turkheimer FE, et al. 2010. Emergence of resting state networks in the preterm human brain. *Proc Natl Acad Sci USA* 107(46):20015–20020, PMID: 21041625, <https://doi.org/10.1073/pnas.1007921107>.
 57. de Bie HMA, Boersma M, Adriaanse S, Veltman DJ, Wink AM, Roosendaal SD, et al. 2012. Resting-state networks in awake five- to eight-year old children. *Hum Brain Mapp* 33(5):1189–1201, PMID: 21520347, <https://doi.org/10.1002/hbm.21280>.
 58. Thomson EM, Kumarathasan P, Calderón-Garcidueñas L, Vincent R. 2007. Air pollution alters brain and pituitary endothelin-1 and inducible nitric oxide synthase gene expression. *Environ Res* 105(2):224–233, PMID: 17662977, <https://doi.org/10.1016/j.envres.2007.06.005>.
 59. Eeftens M, Beelen R, Fischer P, Brunekreef B, Meliefste K, Hoek G. 2011. Stability of measured and modelled spatial contrasts in NO₂ over time. *Occup Environ Med* 68(10):765–770, PMID: 21285243, <https://doi.org/10.1136/oem.2010.061135>.
 60. Foraster M, Esnaola M, López-Vicente M, Rivas I, Álvarez-Pedrerol M, Persavento C, et al. 2022. Exposure to road traffic noise and cognitive development in schoolchildren in Barcelona, Spain: a population-based cohort study. *PLoS Med* 19(6):e1004001, PMID: 35653430, <https://doi.org/10.1371/journal.pmed.1004001>.
 61. Rivas I, Donaire-Gonzalez D, Bouso L, Esnaola M, Pandolfi M, de Castro M, et al. 2016. Spatiotemporally resolved black carbon concentration, schoolchildren’s exposure and dose in Barcelona. *Indoor Air* 26(3):391–402, PMID: 25924870, <https://doi.org/10.1111/ina.12214>.
 62. Hutchison RM, Morton JB. 2015. Tracking the brain’s functional coupling dynamics over development. *J Neurosci* 35(17):6849–6859, PMID: 25926460, <https://doi.org/10.1523/JNEUROSCI.4638-14.2015>.
 63. Marusak HA, Calhoun VD, Brown S, Crespo LM, Sala-Hamrick K, Gotlib IH, et al. 2017. Dynamic functional connectivity of neurocognitive networks in children. *Hum Brain Mapp* 38(1):97–108, PMID: 27534733, <https://doi.org/10.1002/hbm.23346>.
 64. Abrol A, Damaraju E, Miller RL, Stephen JM, Claus ED, Mayer AR, et al. 2017. Replicability of time-varying connectivity patterns in large resting state fMRI samples. *Neuroimage* 163:160–176, PMID: 28916181, <https://doi.org/10.1016/j.neuroimage.2017.09.020>.